Divergent Causes of Terrestrial Water Storage Decline Between Drylands and Humid Regions Globally

Linli An, Jida Wang, Jianping Huang, Yadu Pokhrel, Romain Hugonnet, Yoshihide Wada, Denise Cáceres, Hannes Müller Schmied, Chunqiao Song, Etienne Berthier, et al.

▶ **To cite this version:**

Linli An, Jida Wang, Jianping Huang, Yadu Pokhrel, Romain Hugonnet, et al.. Divergent Causes of Terrestrial Water Storage Decline Between Drylands and Humid Regions Globally. Geophysical Research Letters, 2021, 48, ⟨10.1029/2021GL095035⟩. ⟨insu-03671319⟩

HAL Id: insu-03671319

https://insu.hal.science/insu-03671319v1

Submitted on 24 Jun 2022

HAL is a multi-disciplinary open access archive for the deposit and dissemination of scientific research documents, whether they are published or not. The documents may come from teaching and research institutions in France or abroad, or from public or private research centers.

L'archive ouverte pluridisciplinaire **HAL**, est destinée au dépôt et à la diffusion de documents scientifiques de niveau recherche, publiés ou non, émanant des établissements d'enseignement et de recherche français ou étrangers, des laboratoires publics ou privés.

Copyright - All rights reserved

Check for updates

AGU ADVANCING EARTH AND SPACE SCIENCE

Geophysical Research Letters®

RESEARCH LETTER
10.1029/2021GL095035

Divergent Causes of Terrestrial Water Storage Decline Between Drylands and Humid Regions Globally

Linli An[1], Jida Wang[2], Jianping Huang[1], Yadu Pokhrel[3], Romain Hugonnet[4,5,6], Yoshihide Wada[7], Denise Cáceres[8], Hannes Müller Schmied[8,9], Chunqiao Song[10], Etienne Berthier[4], Haipeng Yu[11], and Guolong Zhang[1]

[1]Collaborative Innovation Center for West Ecological Safety, College of Atmospheric Sciences, Lanzhou University, Lanzhou, China, [2]Department of Geography and Geospatial Sciences, Kansas State University, Manhattan, KS, USA, [3]Department of Civil and Environmental Engineering, Michigan State University, East Lansing, MI, USA, [4]LEGOS, Université de Toulouse, CNES, CNRS, IRD, UPS, Toulouse, France, [5]Laboratory of Hydraulics, Hydrology and Glaciology (VAW), ETH Zürich, Zürich, Switzerland, [6]Swiss Federal Institute for Forest, Snow and Landscape Research (WSL), Birmensdorf, Switzerland, [7]International Institute for Applied Systems Analysis, Laxenburg, Austria, [8]Institute of Physical Geography, Goethe University Frankfurt, Frankfurt am Main, Germany, [9]Senckenberg Leibniz Biodiversity and Climate Research Centre (SBiK-F), Frankfurt am Main, Germany, [10]Key Laboratory of Watershed Geographic Sciences, Nanjing Institute of Geography and Limnology, Chinese Academy of Sciences, Nanjing, China, [11]Northwest Institute of Eco-Environment and Resource, Chinese Academy of Sciences, Lanzhou, China

Abstract Declines in terrestrial water storage (TWS) exacerbate regional water scarcity and global sea level rise. Increasing evidence has shown that recent TWS declines are substantial in ecologically fragile drylands, but the mechanism remains unclear. Here, by synergizing satellite observations and model simulations, we quantitatively attribute TWS trends during 2002–2016 in major climate zones to three mechanistic drivers: climate variability, climate change, and direct human activities. We reveal that climate variability had transitory and limited impacts (<20%), whereas warming-induced glacier loss and direct human activities dominate the TWS loss in humid regions (~103%) and drylands (~64%), respectively. In non-glacierized humid areas, climate variability generated regional water gains that offset synchronous TWS declines. Yet in drylands, TWS losses are enduring and more widespread with direct human activities, particularly unsustainable groundwater abstraction. Our findings highlight the substantive human footprints on the already vulnerable arid regions and an imperative need for improved dryland water conservation.

Plain Language Summary Terrestrial water storage (TWS) losses are increasingly prominent in both global and regional scales, particularly in vulnerable drylands. An accurate attribution of TWS changes is essential for the sustainability and conservation of water resources. We provide a comprehensive interpretation of recent satellite-observed TWS changes in each climate zone through quantitative attributions to natural and anthropogenic factors. We found climate change and direct human activities are the dominant drivers of zonal TWS changes but their impacts are considerably divergent between drylands and humid regions. In humid regions, TWS losses are primarily concentrated on glacierized regions and the net TWS budget in the non-glacierized humid regions exhibits an equilibrium. Contrastively, TWS declines in drylands are more widespread and enduring with human groundwater depletion. Our analysis highlights a pressing need for improving water conservation strategies in global drylands.

Linli An and Jida Wang contributed equally.

Key Points:

- Recent zonal terrestrial water storage (TWS) losses are primary results of climate change and human activities, instead of climate variability
- In humid regions, glacier loss fully explains the net TWS decline, meaning a water budget equilibrium in non-glacierized humid regions
- In drylands, widespread TWS losses are mainly attributed to direct human activities

Supporting Information:

Supporting Information may be found in the online version of this article.

Correspondence to:

J. Huang,
hjp@lzu.edu.cn

Citation:

An, L., Wang, J., Huang, J., Pokhrel, Y., Hugonnet, R., Wada, Y., et al. (2021). Divergent causes of terrestrial water storage decline between drylands and humid regions globally. *Geophysical Research Letters*, *48*, e2021GL095035. https://doi.org/10.1029/2021GL095035

Received 28 JUN 2021
Accepted 10 NOV 2021

© 2021. American Geophysical Union. All Rights Reserved.

1. Introduction

Drylands cover more than 40% of the Earth's land surface and play a key role in global carbon sequestration (Schimel, 2010). Drylands are also home to one-third of human population, who constitutes about half of the residents living below the United Nations poverty line (UNEP, 2011). As one of the most environmentally fragile and economically vulnerable regions, drylands are at the margin of sustainability and are often threatened by severe water stress (Huang et al., 2016). Recent studies have shown that many declining hotspots of terrestrial water storage (TWS) (Famiglietti, 2004), an integration of surface waters, glaciers, canopy water, soil moisture, and groundwater, are concentrated on global drylands (Chang et al., 2020; Rodell et al., 2018; Wang et al., 2018). Water depletion in drylands not only triggers a range of adverse effects on the ecosystem health, but also destabilizes the socioeconomic development for their residents (Cosgrove & Loucks, 2015; Gleeson et al., 2012).

The impacts of water depletion in drylands can also spread across broader geographic regions via the hydrologic cycle, surface-air interactions (e.g., the carbon cycle and dust cycle), virtual water trades, and demographic migration (Dalin et al., 2017; Humphrey et al., 2018; Kok et al., 2018). Therefore, an improved understanding of the causation of TWS changes in drylands, especially in a comparative context of humid regions, is essential for our efforts toward global stability and sustainability.

A wide array of processes can perturb regional water balances and lead to negative TWS trends. Some of the most prominent processes are ice sheet diminution (Slater et al., 2021), glacier mass loss (Hugonnet et al., 2021; Zemp et al., 2019), groundwater depletion (Gleeson et al., 2012; Wada et al., 2012), lake shrinkage (Pekel et al., 2016; Wada et al., 2017), and meteorological droughts (Rodell et al., 2018; Thomas et al., 2014). Despite the variety, these processes are manifestations of three primary mechanistic drivers: climate variability, climate change and direct human activities (Chew & Small, 2014; Khandu et al., 2016; Rodell et al., 2018). Climate variability refers to the oscillation of the Earth's natural climate system (e.g., El Niño-Southern Oscillation (ENSO)), and can affect regional TWS through teleconnection with climate variables, particularly precipitation (Liu et al., 2020). The effects of climate variability are usually transient but can also alter TWS trends on multi-year to decadal scales (Reager et al., 2016). In contrast, the impacts of climate change and direct human activities are more secular. A "categorical evidence" of climate change is the worldwide glacier retreat during the past century (Hugonnet et al., 2021; Roe et al., 2017). Meanwhile, global human water use has increased continuously to meet the ever-growing demand, which aggravates the water scarcity in (semi-)arid regions (Wada et al., 2016).

A major challenge for accurate attribution of TWS changes is that effects of the three mechanistic drivers are often intertwined and the relative importance of each driver varies among regions. Disaggregating contributions of each of the primary drivers is critical to evaluating the tradeoff between environmental conservation and social development. However, existing attributions are often spatially constrained or focused on water components rather than driving mechanisms. For example, Rodell et al. (2018) investigated GRACE-observed TWS trends in 34 hotspots, about half of which are distributed in drylands. The TWS trend in each hotspot was attributed to direct human impacts, natural climate variability, or climate change using multi-variable time series comparison and literature analysis rather than explicit water budgeting (Rodell et al., 2018). A more recent study (Chang et al., 2020) employed a process-based land surface model (Noah-MP) to determine the drivers of TWS declines in southwestern North America, Middle East, and the North China. The applied model did not include direct anthropogenic components, and human impacts were instead interpreted as the residual between GRACE observations and Noah-MP simulations. In another study, Wang et al. (2018) demonstrated a widespread TWS decline across the global endorheic system, which is overall consistent with the geographic extent of drylands (Wang, 2020). Although their attribution was on a global scale, the emphasis was given to the contributions of TWS components, instead of climatic and anthropogenic drivers. Hitherto, we still lack a holistic understanding of TWS changes across drylands and a global-scale attribution to their mechanistic drivers.

Here, we synergize multi-source satellite observations and model simulations to provide a comprehensive attribution of the TWS trends during April 2002 to December 2016 in both global drylands and humid regions. Our attribution focuses on drylands, but also includes humid regions as a whole to contrast how TWS changing mechanisms diverge among different climate conditions. To understand the causes of TWS changes and unpick the complex interactions, we apply GRACE-REC datasets (Humphrey & Gudmundsson, 2019) to estimate the impacts of climate variability, employ high-accuracy glacier mass change observations (Hugonnet et al., 2021) to quantify the contributions of climate change, and conducted sensitivity experiments with the WaterGAP2.2d hydrological model (Müller Schmied et al., 2021) to determine the impacts of direct human activities. More details are given in Methods.

2. Materials and Methods

2.1. Study Regions and Period

Our study period, that is, from April 2002 to December 2016, was determined by the overlapping timespan among all used datasets. Similarly, our studied global land area was the spatial intersection of all applied datasets, which exclude Greenland, Antarctica and several large lakes (e.g., the Caspian Sea, the Aral Sea and the Great Lakes) (Figure 1a). The division of climate zones was based on the commonly applied Aridity Index (Feng & Fu, 2013; Middleton & Thomas, 1997), according to which 49% of the land surface was categorized as drylands

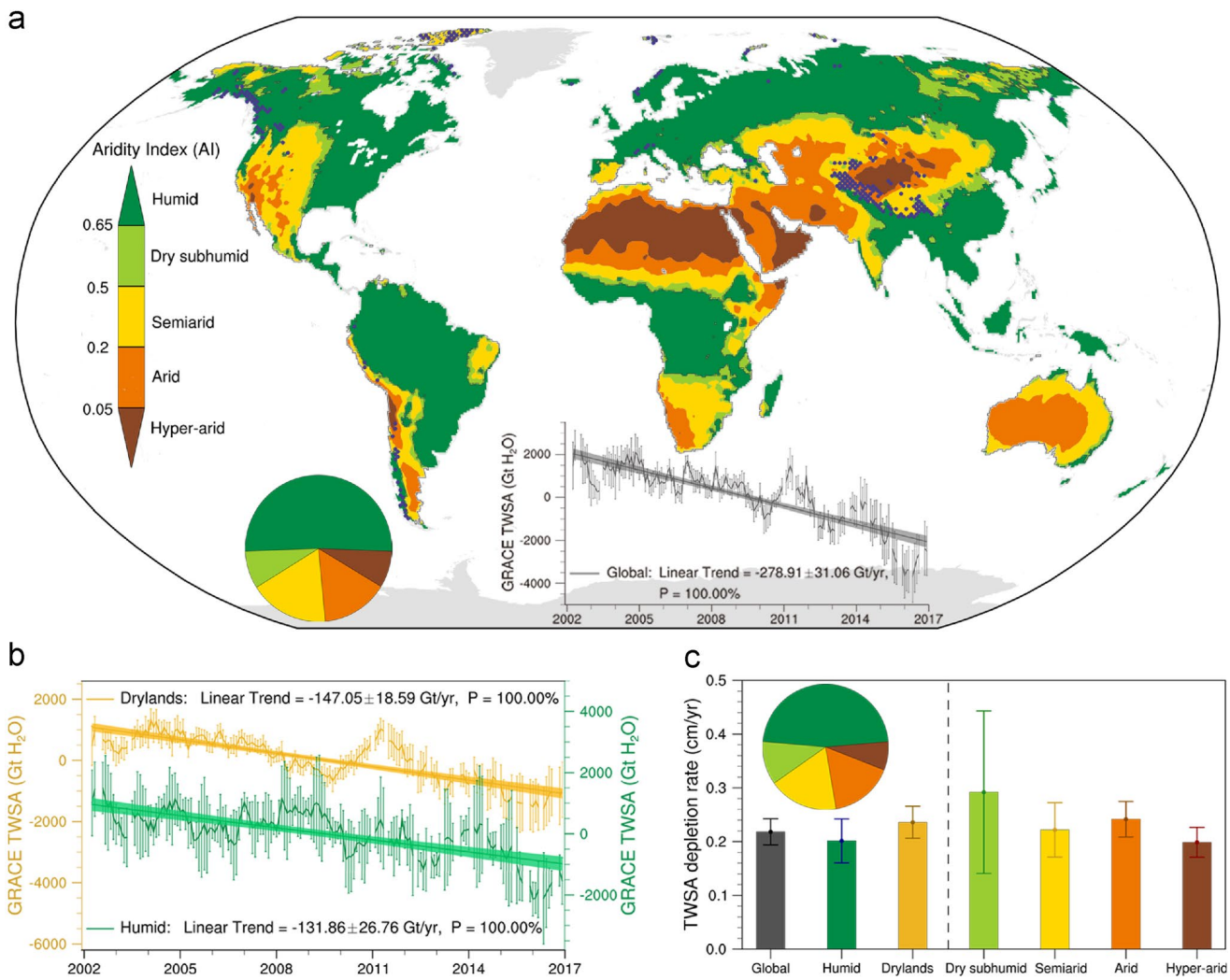

Figure 1. Terrestrial water storage (TWS) trends over different climate zones from GRACE observations, April 2002 to December 2016. (a) Map of climate zones based on the long-term Aridity Index (1961–1990). Blue dots show glacierized regions. The inset pie chart illustrates the proportions of global land area for each climate zone. The inset time series illustrates monthly deseasonalized TWS anomalies in global landmass, with error bars and shading denoting 95% confidence intervals of monthly anomalies and the best-fit linear trend, respectively. (b) Same as the inset time series in (a), but for monthly deseasonalized TWS anomalies in drylands (yellow) and humid regions (green). (c) TWS decline rates (in cm yr^{-1}) for each climate zone. Error bars show 95% confidence intervals. The inset pie chart illustrates the relative contributions of each climate zone to the global TWS change (in Gt yr^{-1}).

and the other 51% as humid regions. Drylands were further divided to hyper-arid (8%), arid (15%), semiarid (18%) and dry subhumid (8%) zones (Figure 1a). See more details in Text 1.1 of Supporting Information S1.

2.2. Quantitative Attributions of GRACE-Observed TWS Trends

TWS trends in each climate zone were quantified using equivalent water thickness (EWT) observations from GRACE satellites (Tapley et al., 2004). We compared the entire collection of GRACE solutions against regional observations, and opted to use the Jet Propulsion Laboratory mascon solution (RL06 v02) (Watkins et al., 2015) for trend calculation and all solutions for uncertainty propagation (Text 1.2 in Supporting Information S1). Then GRACE-observed TWS trends were disaggregated to the contributions of first-order controls or consequences of the three mechanistic drivers: precipitation for climate variability, glacier mass changes for climate change, and water consumption and regulation for direct human activities. Although long-term precipitation trends can be a result of climate change (Skliris et al., 2016), we consider the precipitation fluctuation during the studied 15-year GRACE era mainly a response to inter- and intra-annual climate variability. Precipitation-induced TWS trends

were calculated using the ensemble of the GRACE-REC datasets (Humphrey & Gudmundsson, 2019) (GRACE-REC-EM) which were statistically trained with GRACE measurements and multi-source meteorological forcing (Text 1.3 in Supporting Information S1). Glacier mass changes were derived from fine-spatiotemporal-resolution surface elevation time series over each glacier of the world (Text 1.4 in Supporting Information S1), which were reconstructed from stereo-imagery and validated against high-precision measurements (Hugonnet et al., 2021).

To quantify the impact of direct human activities on TWS trends, we applied the latest version of the state-of-the-art hydrological model WaterGAP2.2d (Text 1.5 in Supporting Information S1), which offers a full representation of human interference directly with the water cycle, including irrigation, reservoir regulation, groundwater abstraction, and multisectoral water use (Müller Schmied et al., 2021). Direct human impacts on TWS and each water component were isolated through sensitivity experiments with WaterGAP2.2d which compared the simulations from a "standard" run considering both climate and human impacts and a "naturalized" run considering no direct human interventions (although land use is included). In addition, we also leveraged the simulated climate-driven TWS changes from WaterGAP2.2d, human water use from the Inter-Sectoral Impact Model Intercomparison Project (Gosling et al., 2017) (ISIMIP) (Text 1.6 in Supporting Information S1), and auxiliary irrigation information (Siebert et al., 2013) (Text 1.7 in Supporting Information S1) to further verify our calculations from GRACE-REC-EM and WaterGAP2.2d and facilitate result interpretations.

3. Results

3.1. Unanimous TWS Declines in Studied Climate Zones

Evident TWS losses have occurred in all studied climate zones during April 2002 through December 2016 (Figure 1). Global humid regions underwent a net TWS change of -131.9 ± 26.8 Gt yr^{-1} (uncertainties are 95% confidence intervals), accounting for ~47% of the concurrent total change (-278.9 ± 31.1 Gt yr^{-1}) in the global landmass (Figure 1). The remaining more than 50% of the global net loss (147.1 ± 18.6 Gt yr^{-1}) stemmed from drylands despite a limited quantity of freshwater resources (Chang et al., 2020; Oki & Kanae, 2006). In global humid regions, the areas that experienced significant TWS loss and gain (with a 0.05 significant level) are overall comparable, but in drylands, the area of significant TWS loss (3.1×10^7 km^2) exceeds that of significant TWS gain (2.2×10^7 km^2) by over 40%. Net TWS losses also prevail in all four dryland climate zones (Figure S3 in Supporting Information S1), each with an area of significant water loss exceeding 50%. These results suggest that although both drylands and humid regions experienced a net TWS decline, the decline in the former was more rapid and widespread.

In addition to a greater TWS loss in the regional total, the average depletion per unit area (or EWT) is slightly more intense in global drylands than in humid regions (Figure 1c). TWS in drylands was depleted at a rate of 2.4 ± 0.3 mm yr^{-1}, which exceeds the rate of 2.0 ± 0.4 mm yr^{-1} in humid regions although the latter hosts the majority of the world's glaciers. Among the four dryland zones, the hyper-arid zone, shows a decreasing rate of 2.0 ± 0.3 mm yr^{-1}. This declining rate is alarming considering that the hyper-arid zone has extremely limited water resources but underwent an EWT loss rate that is comparable to that in global humid regions. The EWT loss rates in the other dryland zones, despite various scales of uncertainty, all exceed that of the humid regions. The arid and semiarid zones suffer from a net TWS loss of 2.4 ± 0.3 mm yr^{-1} and 2.2 ± 0.5 mm yr^{-1}, respectively. The dry subhumid zone has undergone the most intense EWT depletion among the four dryland zones (2.9 ± 1.5 mm yr^{-1}). These unanimous zonal TWS losses not only underscore the severe water depletion in drylands but also imply an imperative need to investigate the causation.

3.2. Limited Impacts of Climate Variability on Zonal TWS Trends

Climate variability exerted limited impacts on TWS trends over each of the climate zones during our studied 15 years (Figures 2a and 2b). As the primary manifestation of inter-annual climate variability, changes of precipitation have led to spatially variable TWS trends at regional levels (Figure S4 in Supporting Information S1). Examples include the wetting Northern Great Plains of North America and Okavango Delta in Africa, and the drying Eastern Brazil and Northwestern Australia (Rodell et al., 2018). However, if aggregating the regional trends over the global non-glacierized landmass, the net impact of precipitation is about 16.7 ± 35.3 Gt yr^{-1}, equivalent to only -6% of the observed global TWS decline (Figures 2a and 2b). In addition to this marginal global impact, precipitation also yields no significant explanation of the observed TWS decline in each climate

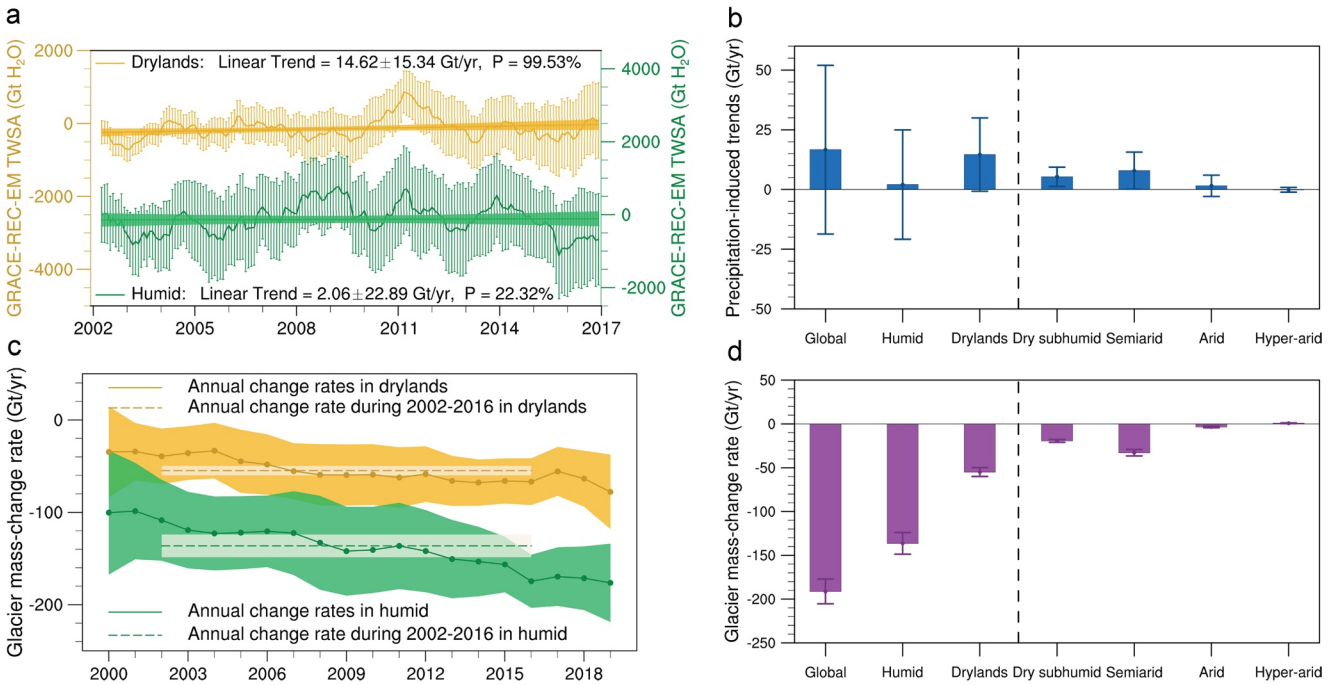

Figure 2. Contributions of precipitation and glaciers to terrestrial water storage (TWS) trends in studied climate zones. (a) Monthly time series of precipitation-induced TWS anomalies in drylands (yellow) and humid regions (green) from April 2002 to December 2016. Error bars and shading illustrate 95% confidence intervals of monthly anomalies and best-fit linear trends, respectively. (b) Precipitation-driven TWS trends in each of the climate zones. (c) Annual time series of glacier mass change rates in drylands (yellow) and humid regions (green). Shading indicates 95% confidence intervals. Dotted horizontal lines denote the 15-year averages (during 2002–2016). (d) Glacier mass change rates in each climate zone.

zone, with a contribution of no more than 15 Gt yr^{-1} or −20% (Figure S5 and Table S1 in Supporting Information S1). These limited contributions are corroborated by the direct observations of precipitation (Figure S6 in Supporting Information S1), and are also consistent with the pattern of ENSO between 2002 and 2016, during which the impacts of major La Niña events during 2008–2014 were largely counteracted by those of the following El Niño (Wang et al., 2018).

Our attribution to climate variability emphasized precipitation, although other climate forcing (e.g., temperature) also influenced the observed TWS trends. To acquire a general scale of the impact of other climate variables, we applied the hydrological model WaterGAP2.2d (Müller Schmied et al., 2021) with full climate forcing (including both precipitation and temperature) to simulate climate-driven TWS changes during the studied 15 years. The simulated TWS trends are comparable to those of GRACE-REC-EM, with their discrepancies within the uncertainty intervals (Figure S7 in Supporting Information S1). This comparison further justified our rationale of using the predominant impact of precipitation to represent the scale of the impact of climate variability on zonal TWS trends.

3.3. Glacier Mass Loss Matches Net TWS Decline in Humid Regions

Our analysis confirms that glacier mass changes, mainly a response to warming climate, explains the net TWS loss across global humid regions (Figures 2c and 2d). Glaciers in humid regions cover 4% (~210,000 km^2) of global humid regions. During 2002 to 2016, the near surface temperature over glacierized regions increased by ~0.6°C (Figure S8 in Supporting Information S1), resulting in a striking glacier mass loss of 136.4 ± 23.8 Gt yr^{-1} in humid regions. Despite a constrained spatial coverage, the total glacier mass loss in humid regions matches its net TWS decline (131.9 ± 26.8 Gt yr^{-1}). In the other 96% of the humid regions, which are not glacierized, climatic and anthropogenic impacts seem to counteract each other, leading to a net TWS equilibrium during the study period. This phenomenon was similarly captured by GRACE observations, where the total area of non-glacierized humid regions with significant drying trends are equivalent to that with wetting trends (Figure S9 in Supporting Information S1).

Unlike the overwhelming influence of climate change in humid regions, glacier retreat explains only about one-third of the TWS decline in global drylands. We calculated a total glacier mass loss of 54.9 ± 5.1 Gt yr^{-1} in drylands from 2002 to 2016. Among the four dryland zones, the semiarid zone, including glaciers in Arctic Canada and part of the glaciers in the HMA, covers the largest glacier extent (~120,000 km^2) and underwent the fastest glacier mass loss at 32.9 ± 3.7 Gt yr^{-1}. In the dry subhumid zone, the glacier mass loss rate is 19.4 ± 1.6 Gt yr^{-1} (Figure 2d). The remaining two zones (i.e., hyper-arid and arid regions) encompass most of the glaciers in central HMA and were affected by the slight mass gain in Karakoram and West Kunlun glaciers, which are the only regions of the world outside the ice sheet peripheries that showed a net glacier accumulation during the past two decades (Farinotti et al., 2020; Hugonnet et al., 2021). As a result, glacier mass changes in these two zones had minuscule contributions (−3.4 ± 0.9 Gt yr^{-1} in the arid zone and 0.7 ± 0.4 Gt yr^{-1} in the hyper-arid zone) to their TWS declines. However, the accelerated glacier mass losses under rising temperature in all dryland climate zones (Figure S10 in Supporting Information S1) suggest that climate change is an increasingly important, albeit not yet dominant, driver of the TWS declines in global drylands.

3.4. Widespread Human Activities Drive Dryland TWS Declines

While climate conditions had driven the recent net TWS decline in humid regions, the widespread water loss across global drylands was attributed predominantly to direct human activities (Figure 3). During the studied 15 years, direct human activities, including human water withdrawals and reservoir management, triggered a total TWS loss of 104.3 ± 5.3 Gt yr^{-1} in the non-glacierized world, more than 90% of which (94.3 ± 3.0 Gt yr^{-1}) originated from drylands. Most of the human-induced TWS loss in drylands is concentrated at regional hotspots where the rate of water consumption exceeds 10 mm yr^{-1} (Figure 3a). Although these consumption hotspots appear sporadic and aggregate to ~4% of the global dryland area, their distribution is widespread, especially in the Northern Hemisphere such as the Arabian Peninsula, western India, northern Sahara, western US, southern Great Plains, and North China Plain. In total, drylands contributed ~86% of the total area of human consumption hotspots in the world. These contrasts signify a disproportionate human footprint and reliance on the already vulnerable dryland ecosystem (Figures 3a and 3b). The substantive TWS decline in drylands stemmed from an unsustainable human water abstraction to meet the growing demands from the irrigation, domestic, industry, and livestock sectors (Table S2 in Supporting Information S1), which increased the regional water outflux through enhanced evapotranspiration (Figure S11 in Supporting Information S1) and ultimately led to dryland TWS declines.

We observed that greater human-induced TWS declines are often accompanied by widespread occurrence of irrigation practices. The semiarid zone, where irrigation area and population are both the largest among the four dryland climate zones (Table S4 and Figure S12b in Supporting Information S1), also underwent the greatest human-induced TWS loss (47.3 ± 2.4 Gt yr^{-1}). This is followed by the arid zone (27.9 ± 0.6 Gt yr^{-1}), the dry subhumid zone (13.3 ± 0.6 Gt yr^{-1}), and the hyper-arid zone (5.7 ± 0.7 Gt yr^{-1}) (Figure 3b), where irrigation area gradually descends (Figure S12b in Supporting Information S1). Compared to the other water use sectors, irrigation is usually more water demanding, and much of the gross water withdrawal is consumed to satisfy the crop biophysiological needs such as transpiration (Pokhrel et al., 2012). This is particularly true in drylands, where the atmospheric water demands are high due to low annual precipitation and the irrigation area in terms of both magnitude and percentage is more pervasive (Figure S12 in Supporting Information S1). For these reasons, although most of the water consumption in industrial and domestic sectors comes from humid regions, irrigation water consumption, which significantly outweighs the total consumption in the other sectors (e.g., by nearly seven times globally), is dominated by global drylands (Tables S2 and S3 in Supporting Information S1). These results suggest that widespread irrigation across drylands is likely the culprit for the excessive TWS decline.

Direct human activities affected the budgets of all water components, but a comprehensive partitioning through hydrological modeling reveals an overwhelming contribution of groundwater depletion on human-induced TWS declines (Figure 3c). Although water regulations in major reservoirs mitigated the global TWS decline by a certain fraction (6.9 ± 4.9 Gt yr^{-1}), the global anthropogenic groundwater depletion reached 111.6 ± 1.0 Gt yr^{-1} from 2002 to 2016, accounting for 40% of the concurrent global net TWS decline (278.9 ± 31.1 Gt yr^{-1}). About 88% of this global groundwater depletion stems from drylands (Figure 3c), meaning that within drylands, human-induced water loss in aquifers alone (98.6 ± 0.9 Gt yr^{-1}) explains nearly 70% of the net TWS decline (147.1 ± 18.6 Gt yr^{-1}). This excessive groundwater depletion in arid climates is overall consistent with previous studies (e.g., Wada et al., 2010; Wang et al., 2018).

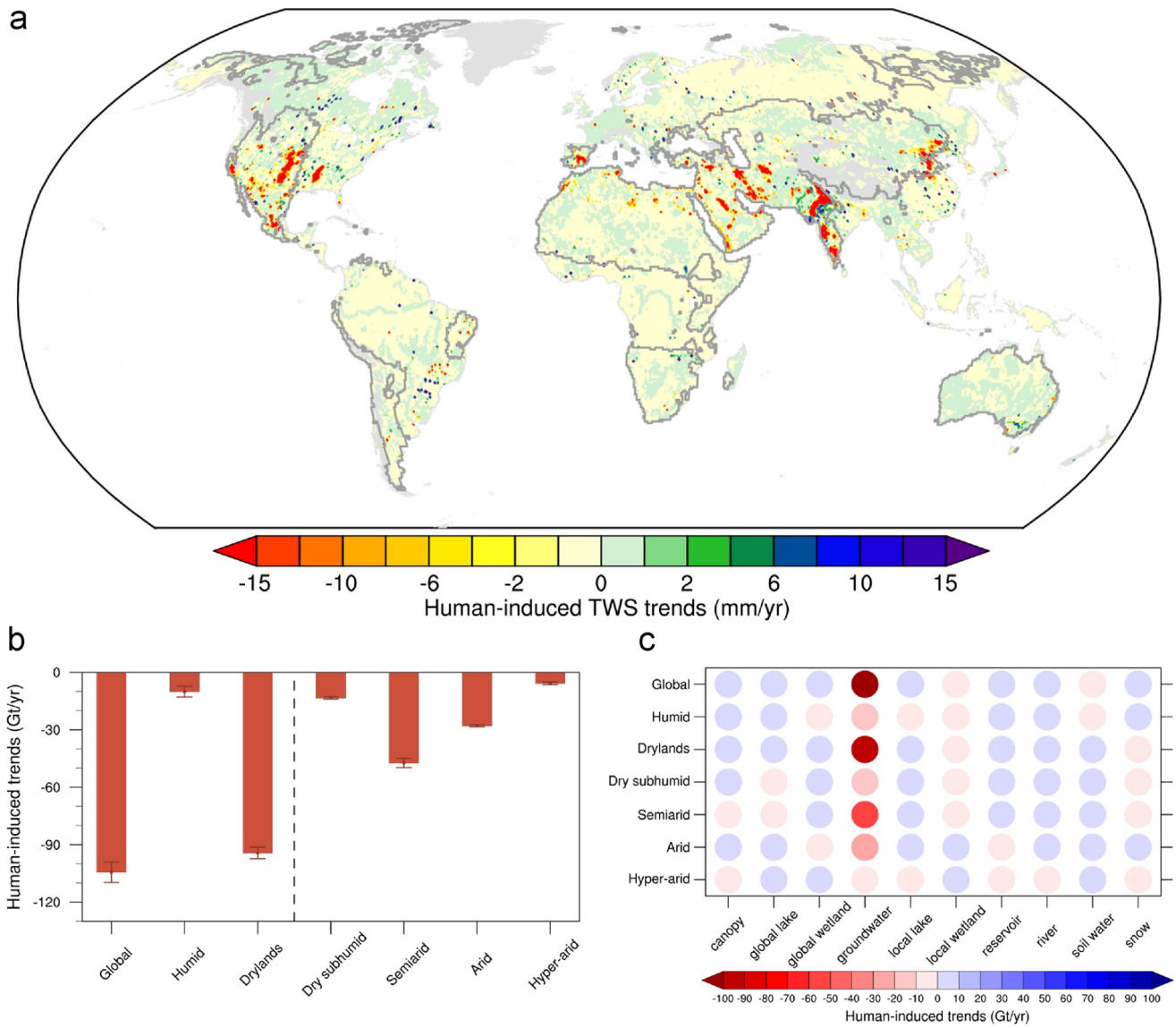

Figure 3. Terrestrial water storage (TWS) trends induced by direct human activities. (a) Global map of human-induced TWS trends simulated by the WaterGAP2.2d hydrological model during April 2002 through December 2016. Lines delineate the extent of global drylands. (b) Human-induced TWS trends in each climate zone. Error bars show 95% confidence intervals. (c) Human-induced TWS trends for different water components in each climate zone (see Table S5 in Supporting Information S1). Glacierized regions are excluded in this result.

This striking dominance of groundwater depletion over dryland TWS declines accentuates the severity of unsustainable water abstraction in arid climates. Limited surface water in drylands, together with their distinct seasonality of precipitation, augmented the societal reliance on groundwater, which in some hyper-arid regions is the only dependable water resource. This is testified by the fact that in each of the dryland zones, the percentage for land area with groundwater-fed irrigation (about 3.0%–6.4%) overpasses the percentage in humid regions (2.0%) (Figure S12a in Supporting Information S1). Meanwhile, aridity leads to extremely low groundwater recharge rates (Döll et al., 2014; Gleeson et al., 2012; Wada et al., 2012). In addition, aquifers in arid and semiarid climates tend to have deeper water tables and can only be recharged following heavy rainfalls or from focused stream leakage (Bierkens & Wada, 2019). All of these situations create a chronic imbalance between water abstraction and recharge and thus deficient budgets in many aquifers across drylands (Richey et al., 2015; Wang et al., 2018). Examples are some of the depletion hotpots in Figure 3, such as in North China, the Indus Basin, and the Arabian Aquifer. To this end, we conclude that despite significant climate impacts on regional water budgets (Chang

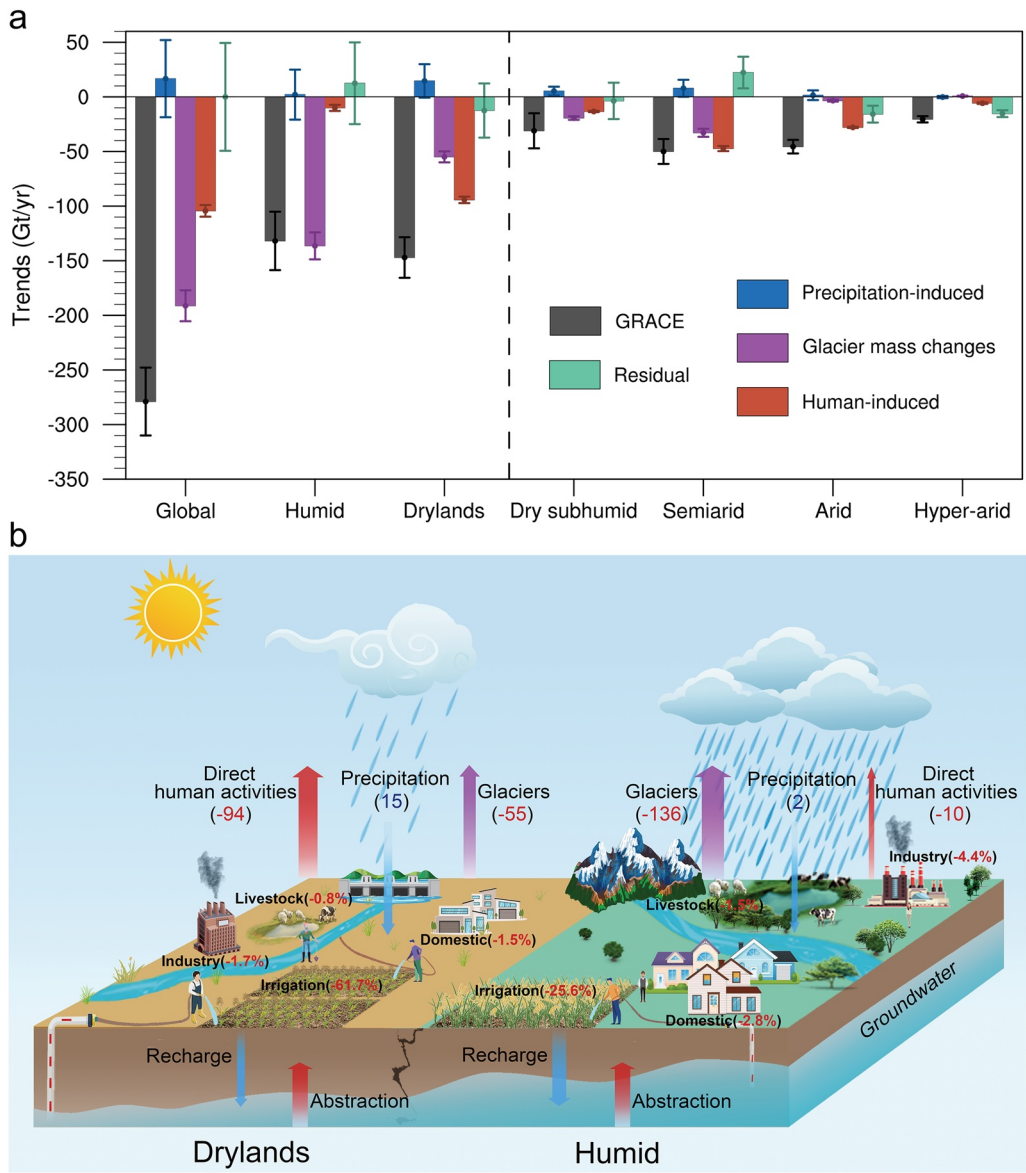

Figure 4. Quantitative attribution of terrestrial water storage (TWS) trends in each climate zone during April 2002 through December 2016. (a) Contributions of each driver to zonal TWS trends (see detailed statistics in Table S1 in Supporting Information S1). (b) Schematic diagram summarizing the contributions of major drivers to the net TWS trends in global drylands and humid regions. Contributions of direct human activities, precipitation, and glacier mass changes are in Gt yr^{-1}, whereas sectoral water consumptions are in percentage (also see Table S6 in Supporting Information S1).

et al., 2020; Rodell et al., 2018; Wang et al., 2018), the net TWS decline in the global drylands is predominately attributed to direct human water-use activities, especially unsustainable groundwater abstraction.

4. Discussions and Implications for Dryland Conservation

Our results provided a comprehensive explanation of the recent zonal TWS changes through a quantitative attribution to climate variability, climate change, and direct human activities (Figure 4 and Table S1 in Supporting Information S1). We showed that climate variability had a limited and transient impact on zonal TWS losses. While the impacts of climate change and direct human activities were more significant and secular, their dominance diverges between humid regions and drylands. Different from the pattern in humid regions, where climate-dom-

inated TWS declines are disproportionally concentrated on glacierized regions, direct human impacts are more widely scattered and aggregate to the primary cause of the water loss in drylands. In addition, we illuminate that the impact of direct human activities on dryland TWS was mainly attributed to excessive groundwater depletions, which resulted in water table declines (Bierkens & Wada, 2019) (Figure 4b) and threatened ecosystems depending on shallow aquifers (Griebler & Avramov, 2015).

As elaborated in Methods, our attribution of the TWS losses was based on an integration of satellite observations and model simulations, and focused on the impacts of primary controls for each of the three mechanistic drivers (i.e., precipitation, glacier mass changes, and human water consumption and regulation). Inevitably, these methods involved a certain degree of simplification and would not perfectly close the GRACE-observed TWS budgets (Figure 4 and Table S1 in Supporting Information S1). While the residuals may imply the scale of the impacts of other controls, such as temperature trend over non-glacierized regions, new reservoir impoundments, and land use land cover changes, they do not seem to alter our major conclusions (see Text 1.8 in Supporting Information S1 for more discussions on residual sources). On the one hand, the residuals for both drylands and humid regions are within their uncertainty intervals. On the other hand, the total residual for drylands is -12.5 Gt yr^{-1}, which slightly undershoots the GRACE-observed trend. As such, a more exhaustive attribution of this residual may further close the gap of the dryland TWS decline, but will not likely oppose the message that direct human activities are the dominant driver for the global dryland water loss.

It is also worth noting that the accuracies of our applied data and model simulation vary in space, leading to an overall reduced capability of attributing TWS variation in smaller domains. For this reason, our attribution was implemented for major climate zones, and caveats should be taken when interpreting our results at finer spatial scales. For experimentation, we replicated the attribution for six regional drylands at continental-to-subcontinental scales (Figure S13 in Supporting Information S1). As expected, the results demonstrate regional variability. The drylands in southern Africa and Australia do not exhibit a net TWS decline. Within other dryland regions, declining TWS signals coexisted with overall weaker water gains (such as in most of sub-Sahara Africa (MacDonald et al., 2021); Figure S9 in Supporting Information S1). Nevertheless, direct human activities remain the dominant driver in most of the dryland regions that experienced a net TWS decline. This is especially true for the Northern Hemisphere, where drylands are both larger and more populated.

Despite inevitable uncertainties, our attribution accentuates the essential importance of decoupling climate-human influences to water resource managements in the ecologically vulnerable drylands. As population and the living standard continue to grow, human water use, which we have quantified to be the major driver of dryland TWS decline, is expected to increase toward the end of this century (Wada & Bierkens, 2014). Although future climate change may alleviate or even reverse the effect of water depletions in some regions, increasing human activities and mismanaged water practice may counteract part of the climate-induced alleviation and further aggravate the water stress in other regions (Pokhrel et al., 2021; Wada et al., 2013, 2016; Wu et al., 2020). This possibility is particularly high in drylands, where the population growth rate is faster (Table S4 in Supporting Information S1) and the ecosystems are more sensitive and fragile. Meanwhile, water scarcity may be amplified by regional warming in drylands (Huang et al., 2017) and further accelerate the degradation of local and surrounding drylands through water and dust cycles (Duniway et al., 2019). Once the land is degraded, the human ecological restoration will require a larger amount of water and result in additional water depletions (Zhao et al., 2020). Given these adverse effects, we suggest immediate adaptation measures, including establishing comprehensive water resource observation systems and developing more effective water management rules, for the disturbed TWS balance in the vulnerable global drylands.

Data Availability Statement

The GRACE Jet Propulsion Laboratory mascon data are available from https://podaac.jpl.nasa.gov/dataset/TELLUS_GRAC-GRFO_MASCON_CRI_GRID_RL06_V2. GRACE-REC datasets are downloaded from https://doi.org/10.6084/m9.figshare.7670849. Glacier mass change estimates are available from https://doi.org/10.6096/13. And the WaterGAP model simulations used in this study are available from https://doi.org/10.1594/PANGAEA.918447.

Acknowledgments
This work was jointly supported by the National Science Foundation of China (41991231, 42041004, and 91937302) and the China University Research Talents Recruitment Program (111 project, No. B13045). The authors acknowledge the ISIMIP project for providing the sectoral human water use datasets. R. Hugonnet acknowledges a fellowship from the University of Toulouse. E. Berthier acknowledges support from the French Space Agency (CNES). The authors thank Fanny Brun (Université Grenoble Alpes) for helping acquire glacier mass change data. The authors thank Taoyong Jin and Xiaolong Li (Wuhan University) for helping calculate the glacier mass change rates from GRACE products. The authors are also grateful for Dr. Robert G. Bryant (University of Sheffield) and another anonymous reviewer for their constructive comments and suggestions, which significantly improved the paper.

References

Bierkens, M. F. P., & Wada, Y. (2019). Non-renewable groundwater use and groundwater depletion: A review. *Environmental Research Letters*, *14*(6), 43. https://doi.org/10.1088/1748-9326/ab1a5f

Chang, L. L., Yuan, R., Gupta, H. V., Winter, C. L., & Niu, G. Y. (2020). Why is the terrestrial water storage in dryland regions declining? A perspective based on gravity recovery and climate experiment satellite observations and Noah land surface model with multiparameterization schemes model simulations. *Water Resources Research*, *56*(11), e2020WR027102. https://doi.org/10.1029/2020wr027102

Chew, C. C., & Small, E. E. (2014). Terrestrial water storage response to the 2012 drought estimated from GPS vertical position anomalies. *Geophysical Research Letters*, *41*(17), 6145–6151. https://doi.org/10.1002/2014gl061206

Cosgrove, W. J., & Loucks, D. P. (2015). Water management: Current and future challenges and research directions. *Water Resources Research*, *51*(6), 4823–4839. https://doi.org/10.1002/2014wr016869

Dalin, C., Wada, Y., Kastner, T., & Puma, M. J. (2017). Groundwater depletion embedded in international food trade. *Nature*, *543*(7647), 700–704. https://doi.org/10.1038/nature21403

Döll, P., Mueller Schmied, H., Schuh, C., Portmann, F. T., & Eicker, A. (2014). Global-scale assessment of groundwater depletion and related groundwater abstractions: Combining hydrological modeling with information from well observations and GRACE satellites. *Water Resources Research*, *50*(7), 5698–5720. https://doi.org/10.1002/2014wr015595

Duniway, M. C., Pfennigwerth, A. A., Fick, S. E., Nauman, T. W., Belnap, J., & Barger, N. N. (2019). Wind erosion and dust from US drylands: A review of causes, consequences, and solutions in a changing world. *Ecosphere*, *10*(3). https://doi.org/10.1002/ecs2.2650

Famiglietti, J. S. (2004). Remote sensing of terrestrial water storage, soil moisture and surface waters. *State of the Planet: Frontiers and Challenges in Geophysics*, *150*, 197–207. https://doi.org/10.1029/150gm16

Farinotti, D., Immerzeel, W. W., de Kok, R., Quincey, D. J., & Dehecq, A. (2020). Manifestations and mechanisms of the Karakoram glacier Anomaly. *Nature Geoscience*, *13*(1), 8–16. https://doi.org/10.1038/s41561-019-0513-5

Feng, S., & Fu, Q. (2013). Expansion of global drylands under a warming climate. *Atmospheric Chemistry and Physics*, *13*(19), 10081–10094. https://doi.org/10.5194/acp-13-10081-2013

Gleeson, T., Wada, Y., Bierkens, M. F., & van Beek, L. P. (2012). Water balance of global aquifers revealed by groundwater footprint. *Nature*, *488*(7410), 197–200. https://doi.org/10.1038/nature11295

Gosling, S., Müller Schmied, H., Betts, R., Chang, J., Ciais, P., Dankers, R., et al. (2017). *ISIMIP2a simulation data from water (global) sector*. GFZ Data Services. https://doi.org/10.5880/PIK.2017.010

Griebler, C., & Avramov, M. (2015). Groundwater ecosystem services: A review. *Freshwater Science*, *34*(1), 355–367. https://doi.org/10.1086/679903

Huang, J., Yu, H., Dai, A., Wei, Y., & Kang, L. (2017). Drylands face potential threat under 2°C global warming target. *Nature Climate Change*, *7*(6), 417–422. https://doi.org/10.1038/nclimate3275

Huang, J., Yu, H., Guan, X., Wang, G., & Guo, R. (2016). Accelerated dryland expansion under climate change. *Nature Climate Change*, *6*(2), 166–171. https://doi.org/10.1038/nclimate2837

Hugonnet, R., McNabb, R., Berthier, E., Menounos, B., Nuth, C., Girod, L., et al. (2021). Accelerated global glacier mass loss in the early twenty-first century. *Nature*, *592*(7856), 726–731. https://doi.org/10.1038/s41586-021-03436-z

Humphrey, V., & Gudmundsson, L. (2019). GRACE-REC: A reconstruction of climate-driven water storage changes over the last century. *Earth System Science Data*, *11*(3), 1153–1170. https://doi.org/10.5194/essd-11-1153-2019

Humphrey, V., Zscheischler, J., Ciais, P., Gudmundsson, L., Sitch, S., & Seneviratne, S. I. (2018). Sensitivity of atmospheric CO_2 growth rate to observed changes in terrestrial water storage. *Nature*, *560*(7720), 628–631. https://doi.org/10.1038/s41586-018-0424-4

Khandu, Forootan, E., Schumacher, M., Awange, J. L., & Muller Schmied, H. (2016). Exploring the influence of precipitation extremes and human water use on total water storage (TWS) changes in the Ganges-Brahmaputra-Meghna River Basin. *Water Resources Research*, *52*(3), 2240–2258. https://doi.org/10.1002/2015wr018113

Kok, J. F., Ward, D. S., Mahowald, N. M., & Evan, A. T. (2018). Global and regional importance of the direct dust-climate feedback. *Nature Communications*, *9*(1), 241. https://doi.org/10.1038/s41467-017-02620-y

Liu, X., Feng, X., Ciais, P., & Fu, B. (2020). Widespread decline in terrestrial water storage and its link to teleconnections across Asia and eastern Europe. *Hydrology and Earth System Sciences*, *24*(7), 3663–3676. https://doi.org/10.5194/hess-24-3663-2020

MacDonald, A. M., Lark, R. M., Taylor, R. G., Abiye, T., Fallas, H. C., Favreau, G., et al. (2021). Mapping groundwater recharge in Africa from ground observations and implications for water security. *Environmental Research Letters*, *16*(3), 034012. https://doi.org/10.1088/1748-9326/abd661

Middleton, N., & Thomas, D. (1997). *World atlas of desertification*. Oxford Univesity Press.

Müller Schmied, H., Cáceres, D., Eisner, S., Flörke, M., Herbert, C., Niemann, C., et al. (2021). The global water resources and use model WaterGAP v2.2d: Model description and evaluation. *Geoscientific Model Development*, *14*(2), 1037–1079. https://doi.org/10.5194/gmd-14-1037-2021

Oki, T., & Kanae, S. (2006). Global hydrological cycles and world water resources. *Science*, *313*(5790), 1068–1072. https://doi.org/10.1126/science.1128845

Pekel, J.-F., Cottam, A., Gorelick, N., & Belward, A. S. (2016). High-resolution mapping of global surface water and its long-term changes. *Nature*, *540*(7633), 418–422. https://doi.org/10.1038/nature20584

Pokhrel, Y., Felfelani, F., Satoh, Y., Boulange, J., Burek, P., Gadeke, A., et al. (2021). Global terrestrial water storage and drought severity under climate change. *Nature Climate Change*, *11*(3), 226–233. https://doi.org/10.1038/s41558-020-00972-w

Pokhrel, Y., Hanasaki, N., Koirala, S., Cho, J., Yeh, P. J. F., Kim, H., et al. (2012). Incorporating anthropogenic water regulation modules into a land surface model. *Journal of Hydrometeorology*, *13*(1), 255–269. https://doi.org/10.1175/Jhm-D-11-013.1

Reager, J. T., Gardner, A. S., Famiglietti, J. S., Wiese, D. N., Eicker, A., & Lo, M. H. (2016). A decade of sea level rise slowed by climate-driven hydrology. *Science*, *351*(6274), 699–703. https://doi.org/10.1126/science.aad8386

Richey, A. S., Thomas, B. F., Lo, M. H., Reager, J. T., Famiglietti, J. S., Voss, K., et al. (2015). Quantifying renewable groundwater stress with GRACE. *Water Resources Research*, *51*(7), 5217–5238. https://doi.org/10.1002/2015wr017349

Rodell, M., Famiglietti, J. S., Wiese, D. N., Reager, J. T., Beaudoing, H. K., Landerer, F. W., & Lo, M. H. (2018). Emerging trends in global freshwater availability. *Nature*, *557*(7707), 651–659. https://doi.org/10.1038/s41586-018-0123-1

Roe, G. H., Baker, M. B., & Herla, F. (2017). Centennial glacier retreat as categorical evidence of regional climate change. *Nature Geoscience*, *10*(2), 95–99. https://doi.org/10.1038/Ngeo2863

Schimel, D. S. (2010). Drylands in the earth system. *Science*, *327*(5964), 418–419. https://doi.org/10.1126/science.1184946

Siebert, S., Henrich, V., Frenken, K., & Burke, J. (2013). *Global map of irrigation areas version 5*. Rheinische Friedrich-Wilhelms-University and Food and Agriculture Organization of the United Nations.

Skliris, N., Zika, J. D., Nurser, G., Josey, S. A., & Marsh, R. (2016). Global water cycle amplifying at less than the Clausius-Clapeyron rate. *Scientific Reports*, *6*, 38752. https://doi.org/10.1038/srep38752

Slater, T., Lawrence, I. R., Otosaka, I. N., Shepherd, A., Gourmelen, N., Jakob, L., et al. (2021). Review article: Earth's ice imbalance. *Cryosphere*, *15*(1), 233–246. https://doi.org/10.5194/tc-15-233-2021

Tapley, B. D., Bettadpur, S., Ries, J. C., Thompson, P. F., & Watkins, M. M. (2004). GRACE measurements of mass variability in the Earth system. *Science*, *305*(5683), 503–505. https://doi.org/10.1126/science.1099192

Thomas, A. C., Reager, J. T., Famiglietti, J. S., & Rodell, M. (2014). A GRACE-based water storage deficit approach for hydrological drought characterization. *Geophysical Research Letters*, *41*(5), 1537–1545. https://doi.org/10.1002/2014gl059323

UNEP. (2011). *Global drylands: A UN system-wide response*.

Wada, Y., & Bierkens, M. F. P. (2014). Sustainability of global water use: Past reconstruction and future projections. *Environmental Research Letters*, *9*(10), 104003. https://doi.org/10.1088/1748-9326/9/10/104003

Wada, Y., Florke, M., Hanasaki, N., Eisner, S., Fischer, G., Tramberend, S., et al. (2016). Modeling global water use for the 21st century: The Water Futures and Solutions (WFaS) initiative and its approaches. *Geoscientific Model Development*, *9*(1), 175–222. https://doi.org/10.5194/gmd-9-175-2016

Wada, Y., Reager, J. T., Chao, B. F., Wang, J., Lo, M.-H., Song, C., et al. (2017). Recent changes in land water storage and its contribution to sea level variations. *Surveys in Geophysics*, *38*(1), 131–152. https://doi.org/10.1007/s10712-016-9399-6

Wada, Y., van Beek, L. P. H., & Bierkens, M. F. P. (2012). Nonsustainable groundwater sustaining irrigation: A global assessment. *Water Resources Research*, *48*(6), W00L06. https://doi.org/10.1029/2011wr010562

Wada, Y., van Beek, L. P. H., van Kempen, C. M., Reckman, J. W. T. M., Vasak, S., & Bierkens, M. F. P. (2010). Global depletion of groundwater resources. *Geophysical Research Letters*, *37*(20), L20402. https://doi.org/10.1029/2010gl044571

Wada, Y., van Beek, L. P. H., Wanders, N., & Bierkens, M. F. P. (2013). Human water consumption intensifies hydrological drought worldwide. *Environmental Research Letters*, *8*(3), 034036. https://doi.org/10.1088/1748-9326/8/3/034036

Wang, J. (2020). Endorheic water. *International Encyclopedia of Geography: People, the Earth, Environment and Technology*. The American Association of Geographers; John Wiley & Sons, Ltd. https://doi.org/10.1002/9781118786352.wbieg2001

Wang, J., Song, C., Reager, J. T., Yao, F., Famiglietti, J. S., Sheng, Y., et al. (2018). Recent global decline in endorheic basin water storages. *Nature Geoscience*, *11*(12), 926–932. https://doi.org/10.1038/s41561-018-0265-7

Watkins, M. M., Wiese, D. N., Yuan, D.-N., Boening, C., & Landerer, F. W. (2015). Improved methods for observing Earth's time variable mass distribution with GRACE using spherical cap mascons. *Journal of Geophysical Research: Solid Earth*, *120*(4), 2648–2671. https://doi.org/10.1002/2014jb011547

Wu, W. Y., Lo, M. H., Wada, Y., Famiglietti, J. S., Reager, J. T., Yeh, P. J., et al. (2020). Divergent effects of climate change on future groundwater availability in key mid-latitude aquifers. *Nature Communications*, *11*(1), 3710. https://doi.org/10.1038/s41467-020-17581-y

Zemp, M., Huss, M., Thibert, E., Eckert, N., McNabb, R., Huber, J., et al. (2019). Global glacier mass changes and their contributions to sea-level rise from 1961 to 2016. *Nature*, *568*(7752), 382–386. https://doi.org/10.1038/s41586-019-1071-0

Zhao, M., G, A., Zhang, J., Velicogna, I., Liang, C., & Li, Z. (2020). Ecological restoration impact on total terrestrial water storage. *Nature Sustainability*, *4*(1), 56–62. https://doi.org/10.1038/s41893-020-00600-7

References From the Supporting Information

Adler, R. F., Huffman, G. J., Chang, A., Ferraro, R., Xie, P.-P., Janowiak, J., et al. (2003). The version-2 global precipitation climatology project (GPCP) monthly precipitation analysis (1979–Present). *Journal of Hydrometeorology*, *4*(6), 11472–1167. https://doi.org/10.1175/1525-7541(2003)004<1147:TVGPCP>2.0.CO

Cáceres, D., Marzeion, B., Malles, J. H., Gutknecht, B. D., Müller Schmied, H., & Döll, P. (2020). Assessing global water mass transfers from continents to oceans over the period 1948–2016. *Hydrology and Earth System Sciences*, *24*(10), 4831–4851. https://doi.org/10.5194/hess-24-4831-2020

Center for International Earth Science Information Network - CIESIN - Columbia University. (2018). *Gridded Population of the World, Version 4 (GPWv4): Population Count, Revision 11*. NASA Socioeconomic Data and Applications Center (SEDAC). https://doi.org/10.7927/H4JW8BX5

Chen, M. Y., Xie, P. P., Janowiak, J. E., & Arkin, P. A. (2002). Global land precipitation: A 50-yr monthly analysis based on gauge observations. *Journal of Hydrometeorology*, *3*(3), 2492–266. https://doi.org/10.1175/1525-7541(2002)003<0249:GLPAYM>2.0.CO

Döll, P., Douville, H., Güntner, A., Müller Schmied, H., & Wada, Y. (2016). Modelling freshwater resources at the global scale: Challenges and prospects. *Surveys in Geophysics*, *37*(2), 195–221. https://doi.org/10.1007/s10712-015-9343-1

Fan, Y., & van den Dool, H. (2008). A global monthly land surface air temperature analysis for 1948–present. *Journal of Geophysical Research*, *113*(D1). https://doi.org/10.1029/2007jd008470

Hanasaki, N., Kanae, S., Oki, T., Masuda, K., Motoya, K., Shirakawa, N., et al. (2008a). An integrated model for the assessment of global water resources - Part 1: Model description and input meteorological forcing. *Hydrology and Earth System Sciences*, *12*(4), 1007–1025. https://doi.org/10.5194/hess-12-1007-2008

Hanasaki, N., Kanae, S., Oki, T., Masuda, K., Motoya, K., Shirakawa, N., et al. (2008b). An integrated model for the assessment of global water resources - Part 2: Applications and assessments. *Hydrology and Earth System Sciences*, *12*(4), 1027–1037. https://doi.org/10.5194/hess-12-1027-2008

Huss, M. (2013). Density assumptions for converting geodetic glacier volume change to mass change. *Cryosphere*, *7*(3), 877–887. https://doi.org/10.5194/tc-7-877-2013

Jin, T., Li, X., Shum, C. K., Ding, H., & Xu, X. (2020). The balance and abnormal increase of global ocean mass change from land using GRACE. *Earth and Space Science*, *7*(5). https://doi.org/10.1029/2020ea001104

Landerer, F. W., & Swenson, S. C. (2012). Accuracy of scaled GRACE terrestrial water storage estimates. *Water Resources Research*, *48*(4). https://doi.org/10.1029/2011wr011453

Luthcke, S., Sabaka, T., Loomis, B., Arendt, A., McCarthy, J., & Camp, J. (2017). Antarctica, Greenland and Gulf of Alaska land-ice evolution from an iterated GRACE global mascon solution. *Journal of Glaciology*, *59*(216), 613–631. https://doi.org/10.3189/2013JoG12J147

Pokhrel, Y., Koirala, S., Yeh, P. J. F., Hanasaki, N., Longuevergne, L., Kanae, S., & Oki, T. (2015). Incorporation of groundwater pumping in a global Land Surface Model with the representation of human impacts. *Water Resources Research*, *51*(1), 78–96. https://doi.org/10.1002/2014wr015602

RGI Consortium. (2017). *Randolph Glacier Inventory – A Dataset of Global Glacier Outlines: Version 6.0: Technical ReportGlobal Land Ice Measurements from Space*. https://doi.org/10.7265/N5-RGI-60

Rost, S., Gerten, D., Bondeau, A., Lucht, W., Rohwer, J., & Schaphoff, S. (2008). Agricultural green and blue water consumption and its influence on the global water system. *Water Resources Research*, *44*(9). https://doi.org/10.1029/2007wr006331

Save, H., Bettadpur, S., & Tapley, B. D. (2016). High-resolution CSR GRACE RL05 mascons. *Journal of Geophysical Research-Solid Earth*, *121*(10), 7547–7569. https://doi.org/10.1002/2016jb013007

Scanlon, B. R., Zhang, Z., Rateb, A., Sun, A., Wiese, D., Save, H., et al. (2019). Tracking seasonal fluctuations in land water storage using global models and GRACE satellites. *Geophysical Research Letters*, *46*(10), 5254–5264. https://doi.org/10.1029/2018gl081836

Scanlon, B. R., Zhang, Z., Save, H., Sun, A. Y., Muller Schmied, H., van Beek, L. P. H., et al. (2018). Global models underestimate large decadal declining and rising water storage trends relative to GRACE satellite data. *Proceedings of the National Academy of Sciences*, *115*(6), E1080–E1089. https://doi.org/10.1073/pnas.1704665115

Schneider, U., Becker, A., Finger, P., Meyer-Christoffer, A., Rudolf, B., & Ziese, M. (2018). *GPCC Full Data Reanalysis Version 8.0 at 0.5°: Monthly land-surface precipitation from rain-gauges built on GTS-based and historic data*. https://doi.org/10.5676/DWD_GPCC/FD_M_V7_050

Sitch, S., Smith, B., Prentice, I. C., Arneth, A., Bondeau, A., Cramer, W., et al. (2003). Evaluation of ecosystem dynamics, plant geography and terrestrial carbon cycling in the LPJ dynamic global vegetation model. *Global Change Biology*, *9*(2), 161–185. https://doi.org/10.1046/j.1365-2486.2003.00569.x

Swenson, S., & Wahr, J. (2006). Post-processing removal of correlated errors in GRACE data. *Geophysical Research Letters*, *33*(8). https://doi.org/10.1029/2005gl025285

Veldkamp, T. I. E., Zhao, F., Ward, P. J., de Moel, H., Aerts, J. C. J. H., Schmied, H. M., et al. (2018). Human impact parameterizations in global hydrological models improve estimates of monthly discharges and hydrological extremes: A multi-model validation study. *Environmental Research Letters*, *13*(5), 055008. https://doi.org/10.1088/1748-9326/aab96f

Wada, Y., Bierkens, M. F. P., de Roo, A., Dirmeyer, P. A., Famiglietti, J. S., Hanasaki, N., et al. (2017). Human–water interface in hydrological modelling: Current status and future directions. *Hydrology and Earth System Sciences*, *21*(8), 4169–4193. https://doi.org/10.5194/hess-21-4169-2017

Wada, Y., Wisser, D., & Bierkens, M. F. P. (2014). Global modeling of withdrawal, allocation and consumptive use of surface water and groundwater resources. *Earth System Dynamics*, *5*(1), 15–40. https://doi.org/10.5194/esd-5-15-2014

Wahr, J., Molenaar, M., & Bryan, F. (1998). Time variability of the Earth's gravity field: Hydrological and oceanic effects and their possible detection using GRACE. *Journal of Geophysical Research*, *103*(B12), 30205–30229. https://doi.org/10.1029/98jb02844

Wang, J., Sheng, Y., & Wada, Y. (2017). Little impact of Three Gorges Dam on recent decadal lake decline across China's Yangtze Plain. *Water Resources Research*, *53*(5), 3854–3877. https://doi.org/10.1002/2016WR019817

Warszawski, L., Frieler, K., Huber, V., Piontek, F., Serdeczny, O., & Schewe, J. (2014). The Inter-Sectoral Impact Model Intercomparison Project (ISI-MIP): Project framework. *Proceedings of the National Academy of Sciences*, *111*(9), 3228–3232. https://doi.org/10.1073/pnas.1312330110

Wiese, D. N., Landerer, F. W., & Watkins, M. M. (2016). Quantifying and reducing leakage errors in the JPL RL05M GRACE mascon solution. *Water Resources Research*, *52*(9), 7490–7502. https://doi.org/10.1002/2016wr019344

Wiese, D. N., Yuan, D.-N., Boening, C., Landerer, F. W., & Watkins, M. M. (2019). *JPL GRACE and GRACE-FO Mascon Ocean, Ice, and Hydrology Equivalent Water Height Coastal Resolution Improvement (CRI) Filtered Release*. https://doi.org/10.5067/TEMSC-3JC62

Xie, P. P., & Arkin, P. A. (1997). Global precipitation: A 17-year monthly analysis based on gauge observations, satellite estimates, and numerical model outputs. *Bulletin of the American Meteorological Society*, *78*(11), 25392–2558. https://doi.org/10.1175/1520-0477(1997)078<2539:GPAYMA>2.0.CO

Zhong, Y., Feng, W., Humphrey, V., & Zhong, M. (2019). Human-induced and climate-driven contributions to water storage variations in the Haihe River Basin, China. *Remote Sensing*, *11*(24). https://doi.org/10.3390/rs11243050